electrostatic repulsion between the two anions.[16] In fact, an esr study by Biloen, *et al.*,[17] has shown the existence of dimers of the type $A^-Me^+A^-$ or $(A^-Me^+)_2$ in solutions of aromatic ions in MTHF. The formation of the activated complex requires desolvation of the cations. The energy required for desolvation is expected to decrease in the series Na^+, K^+, Rb^+, Cs^+,[4] which in part may explain the lowering of E_a (see Table I) with increasing ionic radius. Another factor (discussed in some detail in the recent review by Taube[2]) which will affect the transfer rate is the availability of low-lying empty orbitals in the bridging group. If the metal orbitals play a role in the actual electron transfer, the energy barrier to transfer will decrease in the series Na^+, K^+, Rb^+, Cs^+. Moreover, the more extensive lowest unoccupied orbitals of the larger cations may facilitate their role as an electron conduit by increasing overlap between metal orbitals and π orbitals of the anions.

(16) Note that whereas electron transfer between $A^- \cdot Me^+$ and A is slower than between A^- and A [R. L. Ward and S. I. Weissman, *J. Amer. Chem. Soc.*, **79**, 2086 (1957)], the opposite behavior is expected for transfer between two anions or an anion and dianion.

(17) P. Biloen, R. Prins, J. D. W. van Voorst, and G. J. Hoijtink, *J. Chem. Phys.*, **46**, 4149 (1967).

Acknowledgments. The author is grateful to the Department of Chemistry of MIT for use of their esr equipment. Helpful discussions with Dr. R. I. Gelb are gratefully acknowledged. This work was supported by a grant from the Research Corporation.

Photoinduced Electron Spin Resonance Signals in Acid-Doped Poly(*N*-vinylcarbazole)–Nitroaromatic Charge Transfer Complexes

D. J. Williams,* M. Abkowitz, and G. Pfister

Contribution from the Xerox Corporation, Rochester Research Center, Webster, New York 14580. *Received May 24, 1972*

Abstract: A photoinduced thermally erasable esr signal has been observed in weak charge transfer complexes formed between poly(*N*-vinylcarbazole) (PVCz) and nitroaromatic acceptors such as *o*-dinitrobenzene (DNB) in the presence of strong Brønsted acids such as trichloroacetic acid (TCAA). The time, temperature, and light dependence of the esr signal intensity are found to parallel the electrical conductivity in these systems. The esr signal is attributed to the reversible formation of a protonated nitroaromatic radical anion, *i.e.*, $Ar\text{–}NO_2 \cdot H$, and the electrical conductivity to the simultaneous formation of the mobile positive charge on the radical cation of carbazole. An analysis of the kinetics of these systems shows that the formation of the conductive state occurs *via* a bimolecular reaction between an excited state of the carbazole–nitroaromatic charge transfer complex and a proton. The growth of the esr signal is described over a large time range by $\tanh \beta t$, where β is proportional to the square root of the light intensity, but at short times the growth is much faster. The decay of the signal in the dark follows a second-order rate law. The kinetic model predicts a quadratic growth curve at short times changing into a hyperbolic tangent growth at longer times as well as a bimolecular decay of the conductive state in the dark. Undesirable side reactions accompanied by a discoloration of the materials are accelerated with cyclic light exposure and heating but also occur in the dark and are at least partially attributable to the oxidation of the carbazole ring in the presence of acid. The understanding of the fundamental photo and thermal processes in these materials provides a basis for finding new photoelectric memory effects in organic polymeric solids. These processes constitute a new set of reactions in charge transfer and ion radical chemistry.

Several examples of photoinduced esr signals resulting from irradiation in the charge transfer (CT) absorption band have been reported in the literature. Ilten and Calvin[1] have reported the observation of a reversible photoinduced esr signal and photoconductivity when a solution of tetracyanoethylene (TCNE) in tetrahydrofuran (THF) was irradiated in its CT band. The simultaneous occurrences were attributed to dissociation of the charge transfer triplet state. Recombination of the donor cation radical and acceptor anion radical accounts for loss of the esr signal intensity as well as decay of the photocurrent. Stewart and Eisner[2] observed both a thermal and photoinduced esr signal for TCNE with dimethyl sulfoxide, *N*,*N*-dimethylacetamide, acetone, and THF. Once again the esr signal arises from dissociation of the triplet state in solution, but if the enthalpy of complex formation is sufficiently large the triplet state of the complex will be appreciably populated thermally during complex formation. Esr spectra have also been observed in connection with phosphorescence from CT triplet states. Hayashi, *et al.*,[3] have observed $\Delta M = 2$ transitions for the durene–tetracyanobenzene CT complex triplet state when irradiated in the CT band. A number of other very strong donor acceptor pairs have also been shown to exhibit esr spectra resulting from complete electron transfer and subsequent thermal dissociation of the complex into radical cations and anions in the solid and liquid state.[4–6] The esr signals were

(1) D. F. Ilten and M. Calvin, *J. Chem. Phys.*, **42**, 3760 (1965).
(2) F. Stewart and M. Eisner, *Mol. Phys.*, **12**, 183 (1967).
(3) H. Hayashi, S. Nakagura, and S. I. Iwata, *ibid.*, **13**, 489 (1967).
(4) D. W. Stamires and J. Turkevich, *J. Amer. Chem. Soc.*, **85**, 2557 (1963).

also shown to correlate with electrical conductivity. Thermally populated triplets or triplet ground states also give rise to esr signals but do not produce charge carriers.[7-9] In no cases have reversible photoinduced esr signals been reported for weak donor–acceptor pairs in the solid state.

We have examined the possibility of observing photoinduced esr signals and enhanced electrical conductivity in systems composed of the weak donor polymer poly(*N*-vinylcarbazole) (PVCz) and nitroaromatic acceptors (*i.e.*, *o*-dinitrobenzene (DNB)) and the relatively strong organic acid trichloroacetic acid (TCAA). The excited states of these complexes have relatively large ionic contributions associated with them and may be considered an electrostatically bound cation–anion radical pair. In nitroaromatic anion radicals much of the electron spin density and the charge density is localized on the highly electronegative nitro groups.[10] Nitroaromatic radical anions may therefore act as Brønsted bases and associate with protons. It is therefore reasonable to expect that in the presence of a strong acid such as TCAA the ionic excited state of a weak CT complex may be dissociated into a donor radical cation and proton complexed radical anion.

We have discovered and examined a photoinduced esr signal in such systems and analyzed its behavior as a function of light intensity, time, and concentration of acid. From these data a kinetic model for the chemical and photochemical reactions involved is proposed and tested. The presence of the esr signal is also found to correlate with the conductivity of the material. The esr and kinetic studies will be discussed in this paper, and the detailed electrical measurements and interpretation will be given elsewhere.[11] The results of these experiments elucidate a new set of physical and chemical properties for weak change transfer systems, and the novel electrical properties of the materials are directly attributable to the formation of a metastable complex between a nitroaromatic anion radical and a proton.

Experimental Section

1. Samples. The PVCz (Borden Chemical Co.) was reprecipitated from tetrahydrofuran with methanol and dried in a vacuum oven. A stock solution of PVCz was then prepared in 1,2-dichloroethane. *o*-Dinitrobenzene (K&K Laboratories) was recrystallized from ethanol, and weighed amounts were dissolved in the PVCz stock solution. Trichloroacetic acid was dissolved in 1,2-dichloroethane and added to the PVCz solution immediately before evaporating. The solutions were evaporated *in vacuo* and kept cold in order to avoid side reactions between the PVCz and acid. After thorough drying the samples were ground into fine uniform powders with a mortar and pestle and subsequently packed into quartz esr tubes.

2. Measurements. The esr spectra were obtained in an X-band esr spectrometer operating at 6-KHz modulation. A Varian dual cavity was modified to accept a fiber optics light source by constructing a flange into which the end of the fiber optics bundle could be inserted. The fiber optics were an American Optics incoherent optic bundle with high silicate content glass which highly attenuates light below 4000 Å. A Sylvania DCL 150-W projection lamp was used as the light source. The light intensity was varied using neutral density filters. Figure 1 shows the absorption spectrum of 10-μ thick films of PVCz–DNB–TCAA (25:1:1), PVCz–DNB (24:1), and the transmission spectrum of the light source. The spectra with and without acid are virtually identical. Repeated heating and irradiation caused an irreversible visible discoloration of the films and correspondingly a small broad absorption in the 500–800 nm region of the spectrum appeared.

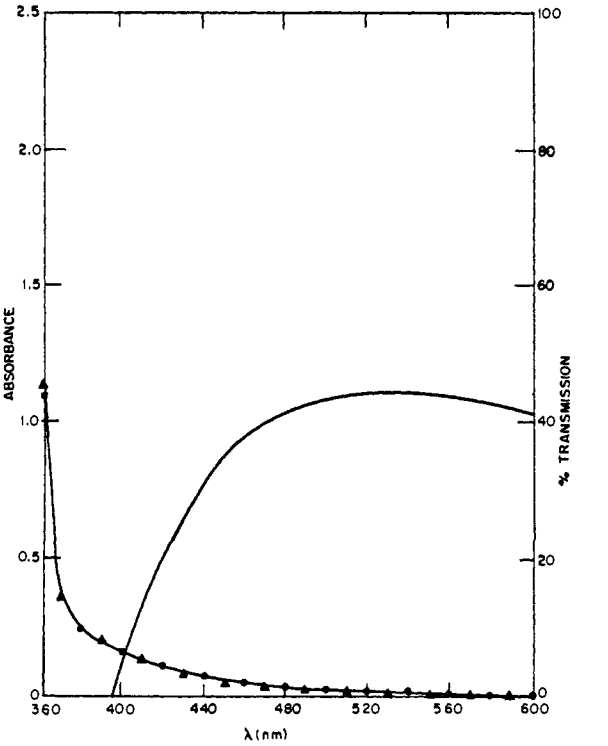

Figure 1. Visible spectrum for 10-μ films of (●) PVCz–DNB–TCAA (24:1:1) and (▲) PVCz–DNB (24:1), and the transmission spectrum of the fiber optics bundle.

The photoinduced esr growth curves were theoretically fitted with a Hewlett–Packard HP9100 calculator–HP-9125B X-Y plotter system. Samples for electrical conductivity measurement were prepared in a sandwich cell configuration by first solvent casting a film of the material from 1,2-dichloroethane on conductive NESA glass and then evaporating a layer of gold on top of the film. The conductivity of the film could then be measured in the dark or after illumination.

Results

The rise in amplitude of the esr signal as a function of time is shown in Figure 2 for the PVCz–DNB–TCAA (24:1:0.8 by weight) system at several light intensities. The experimental intensities were normalized to their respective saturation intensities so that the growth curves are shown normalized to maximum intensity of one. The experimental points have been corrected for a small remnant (thermally irreversible) esr signal whose growth was assumed to be linearly increasing with time. The remnant signal is probably due to oxidation of the carbazole ring which can lead to a variety of paramagnetic and nonparamagnetic colored species,[12,13] *i.e.*, I and II. These species are probably also responsible for the slight increase in absorption in the long wavelength region of the visible spectrum that occurs with cyclic exposing and heating. In the same figure

(5) D. R. Kearns, G. Tollin, and M. Calvin, *J. Chem. Phys.*, **32**, 1020 (1960).
(6) J. W. Eastman, G. M. Androes, and M. Calvin, *ibid.*, **36**, 197 (1962).
(7) D. B. Chesnut and W. P. Phillips, *ibid.*, **35**, 1002 (1961).
(8) D. B. Chesnut and P. A. Arthur, Jr., *ibid.*, **36**, 2969 (1962).
(9) M. T. Jones and D. B. Chesnut, *ibid.*, **38**, 1311 (1963).
(10) K. W. Bowers, "Radical Ions," International Publishers, New York, N. Y., 1968, p 224.
(11) G. Pfister, M. Abkowitz, and D. J. Williams, *J. Chem. Phys.*, in press.
(12) J. F. Ambrose and R. F. Nelson, *J. Electrochem. Soc.*, 1159 (1968).
(13) A. Ledwith and D. F. Iles, *Chem. Commun.*, 498 (1968).

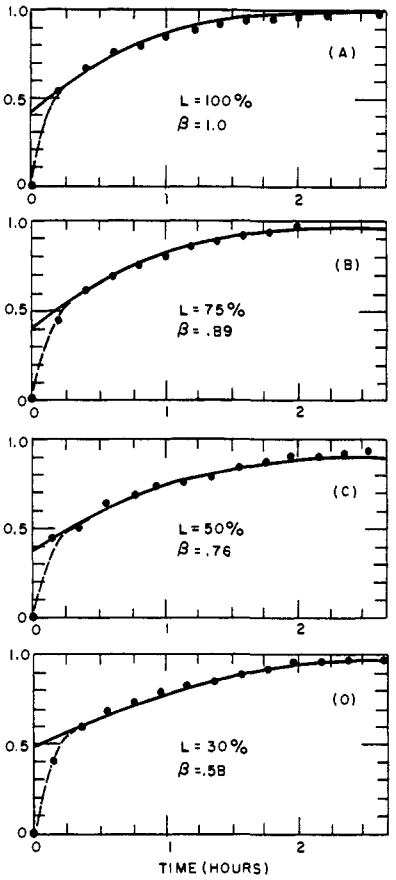

Figure 2. Normalized growth curves (●) for the PVK–DNB–TCAA (24:1:0.8) at (A) 100%, (B) 75%, (C) 50%, and (D) 30% of the maximum light intensity, and the function tanh βt *vs.* time.

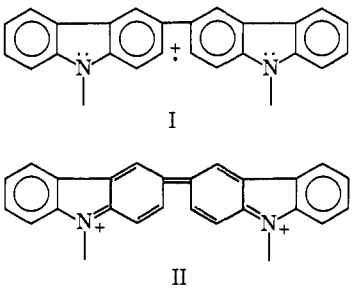

I

II

the function tanh βt is plotted as a function of time. The value of β was chosen to provide the best overall fit with the experimental points. For several minutes following the onset of irradiation the rise of the esr signal intensity is much faster than that obtained using the value of β that best describes the growth of the signal at longer times. The log of the saturation value of the esr signal shows a square-root dependence on the log of the light intensity (L) in Figure 3. On the same graph log β *vs.* log L shows a similar square-root dependence.

The esr signal at two different acid concentrations after 1 hr of illumination is shown in Figure 4. The signal has a peak-to-peak line width of approximately 13 G which is independent of the amplitude and a g value of 2.005. The signal intensity is proportional to the signal amplitude for constant line width. The samples differ in acid concentration by a factor of 4, and the relative intensities of the signal differ by a factor of ~2.

The decay of the inverse esr signal intensity *vs.* time for three different acid concentrations is shown in Figure 5. The samples were irradiated uniformly for 15 min outside the esr tube using a photoflood lamp. The intensity of the esr signal is seen to be a function of the acid concentration. A factor of 100 in acid concentration produced about a tenfold change in initial intensity. The decay of the esr signal exhibits second-order kinetics, and the relative rate constant is independent of acid concentration. The second-order expression for the intensity as a function of time can be written as

$$\frac{1}{I} = k't + \frac{1}{I(0)}$$

where $I(0)$ is the intensity at $t = 0$ and k' is the relative second-order rate constant and is related to the true

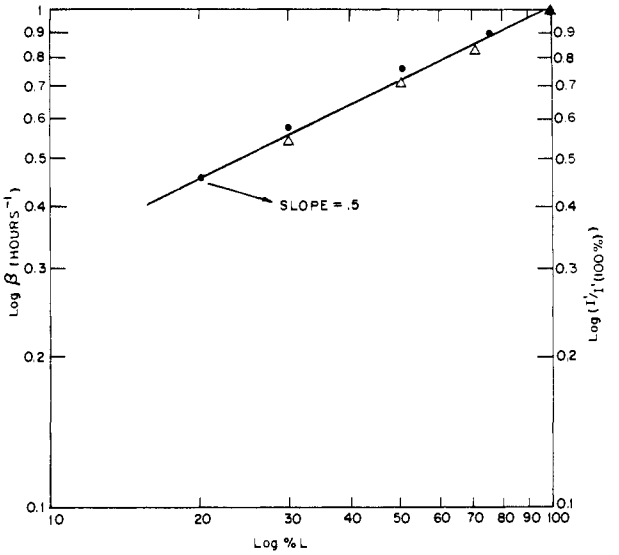

Figure 3. (Δ) A plot of the log of the saturation esr intensity (I') at various values of the light intensity normalized with the saturation signal at maximum light intensity [I' (100%)]. (●) A plot of log β *vs.* log light intensity. The straight line is a calculated square-root dependence of the ordinate on the abscissa.

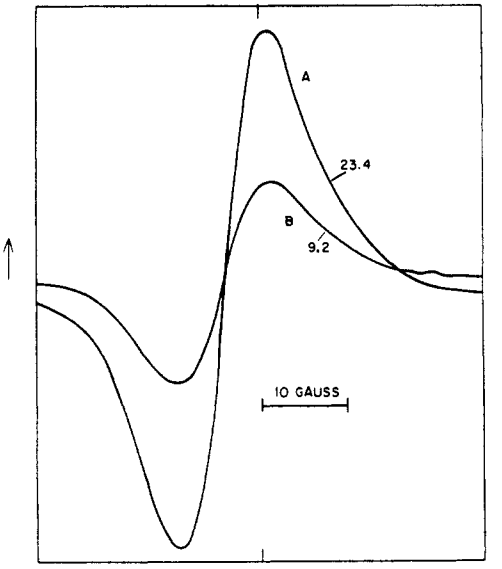

Figure 4. Esr signal for PVK–DNB–TCAA (A) (24:1:0.8) and (B) (24:1:0.2) after 1 hr of illumination. The relative intensities are given.

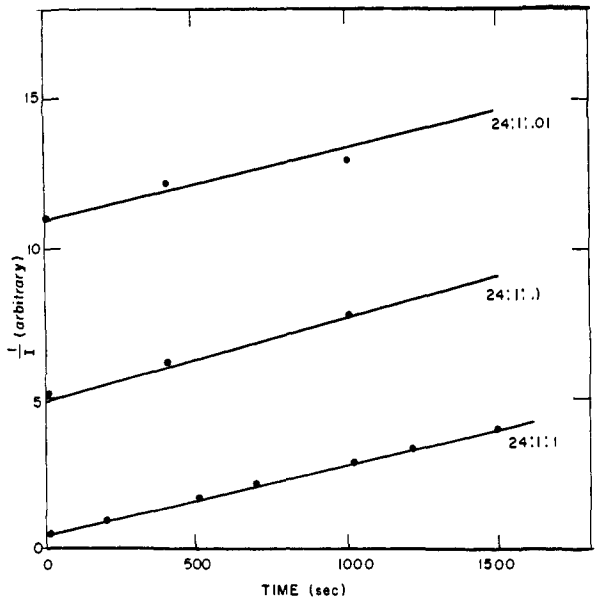

Figure 5. A plot of the inverse relative esr signal intensity *vs.* time for three acid concentrations for PVCz–DNB–TCAA.

rate constant by a conversion factor from esr intensity to concentration. It is convenient to assign an intensity of unity to the esr signal at $t = 0$ (*i.e.*, time at which the illumination is terminated) and examine the decay as a function of temperature. The decay of the esr signal as a function of temperature for the PVCz–DNB–TCAA (24:1:1) system is shown in Figure 6, and the calculated relative second-order rate constants are shown. Arrhenius plots for the system are shown in Figure 7. The activation energy for decay of the light-induced esr signal is about 14 kcal/mol. A large change in dc conductivity following irradiation is always observed to accompany the photogenerated esr signal. Both the enhanced conductivity and esr signal are thermally erasable.

Discussion

The following scheme accounts for the origin and behavior of the esr signal. The acid is partially dissociated according to the equation into a relatively mobile proton and its conjugate base.

$$HB \rightleftharpoons H^+ + B^- \qquad (1)$$

The donor D and acceptor A are in equilibrium with the charge transfer complex DA which can be excited with light (L)

$$D + A \rightleftharpoons DA \qquad (2)$$

$$DA \xrightarrow{L} DA^* \qquad (3)$$

to its first excited singlet state. Singlet state lifetimes are very short, *i.e.*, nanoseconds,[14] and the primary pathways for deactivation are the return to the ground state with the emission of light or thermal energy and intersystem crossing to the triplet state. In addition the excited state may dissociate into the component anion and cation radical in the presence of a strong external perturbation, *i.e.*, electric field, solvation, etc.

$$DA^* \xrightarrow{k_1} DA + \text{energy} \qquad (4)$$

(14) N. J. Turro, "Molecular Photochemistry," W. A. Benjamin, New York, N. Y., 1967, p 49.

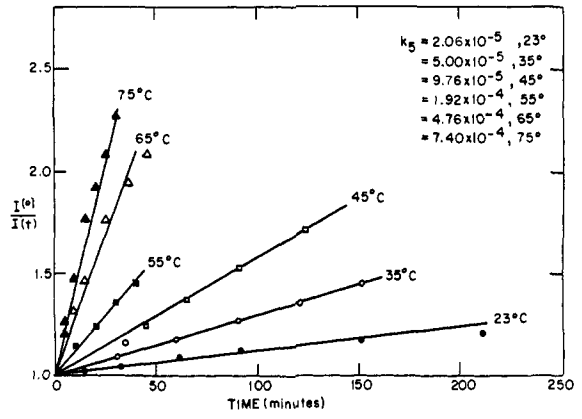

Figure 6. Second-order plot of the decay of the esr signal *vs.* time at several temperatures for PVCz–DNB–TCAA (24:1:1).

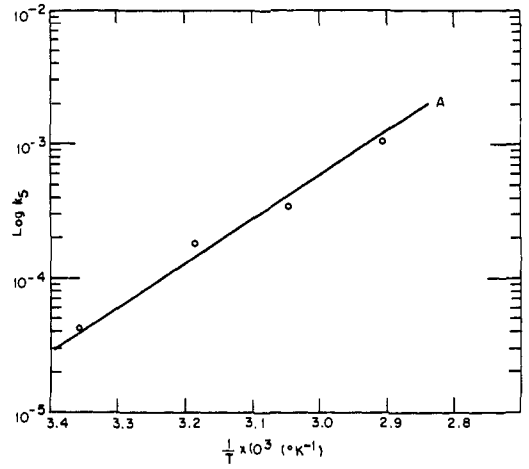

Figure 7. Plot of log k *vs.* $1/T$ for PVCz–DNB–TCAA (24:1:1).

$$DA^* \xrightarrow{k_2} D\cdot^+ + A\cdot^- \qquad (5)$$

and the recombination reaction can be written as

$$D^+ + A\cdot^- \xrightarrow{k_3} DA + \text{energy} \qquad (6)$$

The possibility of an intersystem crossing step exists, but it will be shown that the experimentally verifiable parameters do not distinguish between reactions of the singlet or triplet state. The kinetic analysis is therefore given in terms of reactions of either state represented by DA*. The formation of the long-lived conductive state occurs *via* the unique reaction between the excited state of the complex and a proton.

$$DA^* + H^+ \xrightarrow{k_4} HA\cdot + D\cdot^+ \qquad (7)$$

The species HA· on the right-hand side of eq 7 is postulated as being a protonated anion radical consistent with structure III. The existence of this species

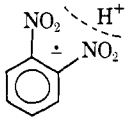

III

in the solid state is based on the acid concentration dependence of the esr spectrum and the observation that the electronic conductivity in the photoinduced state is due to holes,[11] *i.e.*, D·$^+$. It is species III that most

likely gives rise to our esr signal. It is likely that the highly mobile positive charge will lead to line broadening[1,6] of the esr signal from the carbazole radical due to the contribution of spin exchange to the electron spin–spin relaxation time.

The recombination reaction can be postulated as

$$HA\cdot + D\cdot^{+} \xrightarrow{k_5} DA + H^{+} + \text{energy} \quad (8)$$

The actual mechanism for recombination is probably much more complicated and could involve a thermal dissociation of HA· followed by a rate-determining bimolecular reaction between $A\cdot^{-}$ and $D\cdot^{+}$.

For the sake of simplicity in interpreting the esr data, reactions 5 and 6 will be ignored since no external perturbation is present to make either of the reactions appreciable. These reactions must be taken into account, however, in order to interpret the growth of the conductivity under bias and steady-state illumination.

An expression for the concentration of HA· and therefore the esr signal intensity can be written

$$d[HA\cdot]/dt = k_4[DA^*][H^+] - k_5[HA\cdot]^2 \quad (9)$$

When the light incident on the esr cavity is turned off, the concentration of DA* goes to zero and (9) can be rewritten

$$d[HA\cdot]/dt = -k_5[HA\cdot]^2 \quad (10)$$

This corresponds to a second-order decay of the esr signal amplitude which is independent of acid concentration and is in good agreement with the results shown in Figures 5–7.

Equation 9 can be integrated if the concentration of DA* can be obtained. If the singlet state reacts with the proton, its rate of formation will be proportional to the light intensity and

$$d[DA^*]/dt = L - \overbrace{(k_1 + k_2 + k_4[H^+])}^{A}[DA^*] \quad (11)$$

If the singlet state is too short lived to react with the proton and intersystem crossing to the triplet state is appreciable so that the triplet state reacts with the proton and if a steady-state concentration of singlet state is assumed, then the rate of formation of the triplet state would be proportional to L. Equation 11 therefore adequately describes the rate equation for DA* reacting with a proton regardless of whether the singlet or triplet state is involved. An expression for DA* can therefore be obtained by integrating (11).

$$[DA^*] = \frac{L}{A}\left(1 - \frac{1}{L}e^{-At}\right) \quad (12)$$

Substitution in (9) for [DA*] gives

$$\frac{d[HA\cdot]}{dt} = k_4[H^+]\left(\frac{L}{A}\right)\left(1 - \frac{1}{L}e^{-At}\right) - k_5[HA\cdot]^2 \quad (13)$$

At long times when [HA·] reaches its steady-state value

$$\frac{d[HA\cdot]}{dt} \longrightarrow 0 \text{ and } e^{-At} \longrightarrow 0 \quad (14)$$

so that [HA·] and the esr intensity are given by

$$[HA\cdot] = \left[\left(\frac{k_4}{k_5}\right)\frac{L}{A}[H^+]\right]^{1/2} \quad (15)$$

At steady-state or saturation the esr signal should be proportional to the square root of the light intensity.

Figure 3 shows that the experimentally observed saturation amplitude varies as $L^{1/2}$ and agrees well with (15). Also if the reasonable assumption is made that $k_1 + k_2 \gg k_4[H^+]$

$$[HA\cdot] = \left[\frac{k_4[H^+]}{k_5(k_1 + k_3)}\right]^{1/2} \quad (16)$$

and the saturation signal should be approximately proportional to the square root of the acid concentration. This is consistent with the results in Figures 4 and 5.

If (13) is rewritten in the form

$$\frac{d[HA\cdot]}{dt} + k_5[HA\cdot]^2 - \frac{L}{A}\left(1 - \frac{1}{L}e^{-At}\right) = 0 \quad (17)$$

this is an example of Ricotti's equation which is a first-order nonlinear differential equation and cannot be solved in closed form. However, several simplifying assumptions can be made under special conditions. When the light is first turned on $[HA\cdot] \simeq 0$, and integration of (17) gives

$$[HA\cdot] = \frac{L}{A}t - \frac{1}{A}t + t^2 \quad (18)$$

and a quadratic dependence of the esr signal intensity with time is predicted. At large t the term $e^{-At} \rightarrow 0$ and (17) can be written as

$$\frac{d[HA\cdot]}{dt} = \frac{L}{A} - k_5[HA\cdot]^2 \quad (19)$$

and integration gives

$$[HA\cdot] = \left(\frac{L}{k_5 A}\right)^{1/2} \tanh \overbrace{\left(\frac{L}{A}k_5\right)^{1/2}}^{\beta} t \quad (20)$$

The growth curves in Figure 2 comply with (20) for times longer than several minutes. At shorter times the rise in the esr signal intensity is much faster and is consistent with the quadratic dependence predicted by (18) for small values of t. Equation 20 also predicts a square-root dependence of β (coefficient of t in the argument of the hyperbolic tangent) on the light intensity. The plot of $\log \beta$ *vs.* $\log L$ in Figure 2 confirms this square-root dependence. The model therefore appears to be in good agreement with the experimental results.

Conclusions

The observation of a photoinduced thermally reversible esr signal in PCVz–DNB–TCAA has been explained in terms of a reversible reaction between the excited state of the carbazole–nitroaromatic charge transfer complex with a proton. The solutions to the rate equation for HA· were shown to have the same form regardless of whether HA· is formed from a bimolecular reaction of the singlet state or triplet state with a proton. Because of the much longer lifetimes of of triplet states, however, it seems likely that the triplet state is involved.

The nitroaromatic radical anion is apparently a sufficiently strong base to compete for the mobile proton against the (CCl_3COO^-) conjugate base. The rela-

tive stability of the $ArNO_2H\cdot$ type complex is a function of the charge density on the nitro group so that the stability of the complex would be expected to decrease for larger aromatic systems. The proposed kinetic model is in excellent agreement with the observed dependence of the esr signal amplitude on acid concentration, light intensity, and time. The photochemical changes induced in the system account for the observed changes in conductivity assuming that the mobile hole D^+ is the charge carrier. This result is discussed at some length in the paper describing our electrical measurements.[11] The correspondence between the time dependence and thermal behavior of the esr signal and conductivity lend further support to this analysis. The concept of acid–base reactions with the photoexcited state species of a weak charge transfer complex is a new and useful concept and can lead to materials with novel electrical properties.

Electron Spin Resonance Study of Pyrolysis and Photolysis of 2-Iodoacetic Acid and 2-Iodoacetamide

Paul H. Kasai* and D. McLeod, Jr.

Contribution from the Union Carbide Corporation, Tarrytown Technical Center, Tarrytown, New York 10591.
Received May 5, 1972

Abstract: Using rare-gas matrix isolation techniques, esr spectra of the pyrolyzates and photolyzates of 2-iodoacetic acid and 2-iodoacetamide were examined. The results can be summarized as follows. The primary radicals

$$ICH_2COOH \xrightarrow{\Delta} H_2\dot{C}COOH \xrightarrow{\Delta} CH_3 + CO_2$$
$$\xrightarrow{h\nu} 2H\dot{C}O + \dot{H}$$

$$ICH_2CONH_2 \xrightarrow{\Delta} H_2\dot{C}CONH_2 \xrightarrow[\text{or } h\nu]{\Delta} H_2C{=}C{=}O + \dot{N}H_2$$

(the carboxymethyl and the carbamylmethyl radicals) were detected only in low-temperature (300–400°) pyrolysis. The direct photolysis of the iodides produced only the final products.

During the course of our study of substituted phenyl radicals, it became apparent that the 1–3 intramolecular hydrogen transfer occurs quite readily in the case of 2-hydroxyphenyl radicals.[1] The rearrangement which occurs when the precursor *o*-iodophenol is pyrolyzed at ~500°, eventually yields the cyclopentadienyl radicals as shown below.

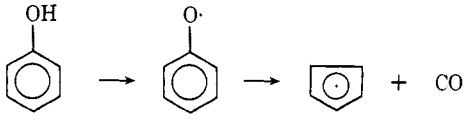

Almost an identical hydrogen transfer was observed when the phenol anion radical was generated within an argon matrix by the photoelectron transfer technique.[2]

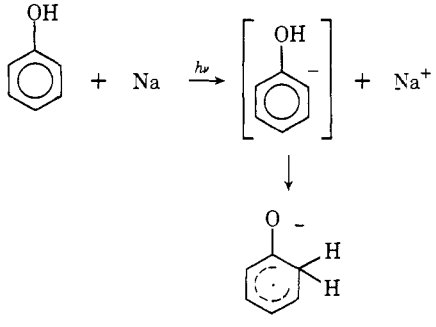

The acidity of the phenolic hydrogen must be the major driving force toward such rearrangements.

In order to examine the generality of the process we studied the pyrolysis and photolysis of 2-iodoacetic acid and 2-iodoacetamide using the esr matrix isolation technique. The carboxymethyl radical $H_2\dot{C}$–COOH should represent the simplest 1–3 system containing an acidic hydrogen. The result confirmed our expectation that the 1–3 hydrogen occurs readily with $H_2\dot{C}$–COOH but to a much lesser extent with $H_2\dot{C}$–$CONH_2$. The experiment also revealed an unexpected photolysis of $H_2\dot{C}$–COOH which results in the formation of the formyl radicals and atomic hydrogen. This report presents and discusses the spectral evidence obtained from these molecules supporting such rearrangement and decomposition processes.

Experimental Section

The description of the liquid-helium cryostat and X-band esr spectrometer system which allows the trapping of transient radicals in an inert gas matrix and the observation of their esr spectra has been reported previously.[3] In the case of pyrolysis the precursors (2-iodoacetic acid and 2-iodoacetamide) were passed through a resistively heated quartz tube and then trapped in an argon or neon matrix being formed upon the cold finger, a flat spatula shaped sapphire rod in contact with the liquid helium reservoir. In the case of photolysis an argon matrix containing the precursor was first prepared and then irradiated with uv light through the side quartz window. A high-pressure mercury arc (GE, AH-6) equipped with a Corning 7-54 uv filter was used for this purpose. The

(1) P. H. Kasai and D. McLeod, Jr., unpublished results.
(2) P. H. Kasai and D. McLeod, Jr., *J. Amer. Chem. Soc.*, **94**, 6872 (1972).
(3) P. H. Kasai, E. Hedaya, and E. B. Whipple, *ibid.*, **91**, 4364 (1969).